CHEMISTRY
A EUROPEAN JOURNAL

DOI: 10.1002/chem.200600591

Characterization of Peptide–Pyrazole Interactions in Solution by Low-Temperature NMR Studies

Wei Wang[a] and Klaus Weisz*[b]

Abstract: Complexation of the amino- and carboxyl-protected tripeptide Piv-L-Val-L-Val-L-Val-*t*Bu with 3-methylpyrazole and 3-amino-5-methylpyrazole was studied by low-temperature NMR experiments in a freonic solvent. The peptide forms an extended β-type structure at all temperatures and associates through hydrogen bonding with the two pyrazole-based β-sheet ligands. A detailed structural characterization of the formed complexes by one- and two-dimensional NMR experiments under slow exchange conditions was made possible by employing very low temperatures. The tripeptide associates to stable antiparallel dimers that are symmetrically capped on both sides by two pyrazole receptors to form 2:2 complexes. Amide groups of two neighboring residues in an extended conformation are involved in cyclic hydrogen bonds to the pyrazole. Based on amide chemical shift changes, the relative strength of intermolecular hydrogen bonds can be assessed and correlated with the electronic effects of the substituents on the pyrazole.

Keywords: hydrogen bonds · molecular recognition · NMR spectroscopy · peptides · pyrazoles

Introduction

Proteins can adopt a wide variety of different structures that enable them to perform their numerous functions in a living cell and determine their intermolecular interactions. Correspondingly, misfolding not only prevents proteins from their correct functioning but may also cause severe pathological conditions in living organisms. These include various neurodegenerative diseases in both animals and humans as a result of uncontrolled protein aggregation.[1] Thus, enzymatic cleavage of amyloid precursor protein can produce amyloid β-peptides that self-aggregate into insoluble fibrils associated with Alzheimer's disease.[2] A structural model of amyloid fibrils indicate β-strand interactions as a major driving force for fibrillogenesis.[3] Though the exact correlation between plaque formation and the onset of the disease is not quite clear yet, the formation of β-amyloid peptide fibrils became a key target in drug development for Alzheimer's disease.[4]

The importance of understanding and controlling peptide interactions has initiated efforts directed towards the development of artificial templates that selectively stabilize and bind to a defined peptide structure.[5] Some time ago, rationally designed nonpeptidic aminopyrazole derivatives have been demonstrated to recognize and bind to dipeptides in a β-sheet conformation by the formation of intermolecular hydrogen bonds to the peptide backbone.[6] This concept has recently been extended to the design of pyrazole receptors bearing additional substituents for the interaction with specific amino acid residues,[7] of dimeric and oligomeric aminopyrazoles for enhanced binding affinity[8] and of chimeric compounds composed of aminopyrazolecarboxylic acids and naturally occurring α-amino acids for sequence-selective protein recognition.[9]

Unfortunately, the characterization of small β-sheet peptide models and their complexation with pyrazole ligands by NMR spectroscopic techniques in solution is limited by the fast dynamics of the systems under investigation. Thus, basic and important parameters such as individual peptide conformers, ligand tautomers, complex geometries and the strength of formed hydrogen bonds are only accessible as averages due to their fast exchange on the NMR time scale. To overcome these shortcomings and to investigate the association and complexation of model peptides in more detail,

[a] Dr. W. Wang
Freie Universität Berlin, Institut für
Organische Chemie, Takustrasse 3, 14195 Berlin (Germany)
[b] Prof. Dr. K. Weisz
Ernst-Moritz-Arndt-Universität
Greifswald, Institut für Chemie und Biochemie
Soldmannstrasse 16, 17487 Greifswald (Germany)
Fax: (+49) 3834-864427
E-mail: weisz@uni-greifswald.de

NMR experiments have to be performed at temperatures low enough to be in the slow motional regime where exchange between species is slow and individual complexes can be studied independently. In the past we have performed such low-temperature NMR experiments on the association of nucleosides by employing a deuterated freonic solvent that allows measurements at temperatures as low as 100 K.[10] In the following we present NMR experiments on the protected tripeptide Piv-L-Val-L-Val-L-Val-*t*Bu and its complexation with pyrazole and aminopyrazole ligands in Freon allowing for the first time a detailed characterization of the formed complexes in solution.

Results and Discussion

Conformational and binding studies at ambient temperatures: For our studies on peptide recognition we employed a Val-Val-Val tripeptide as shown in Figure 1 (top). Because of its bulky side chains, this peptide is expected to adopt a structure close to an extended β-sheet conformation. In order to eliminate interactions due to the terminal functionalities, amino- and carboxyl termini were initially protected by acylation with pivaloyl chloride and by esterification with isobutene.[11,12] These protecting groups also ensured sufficient solubility of the peptide in a freonic solvent mixture.

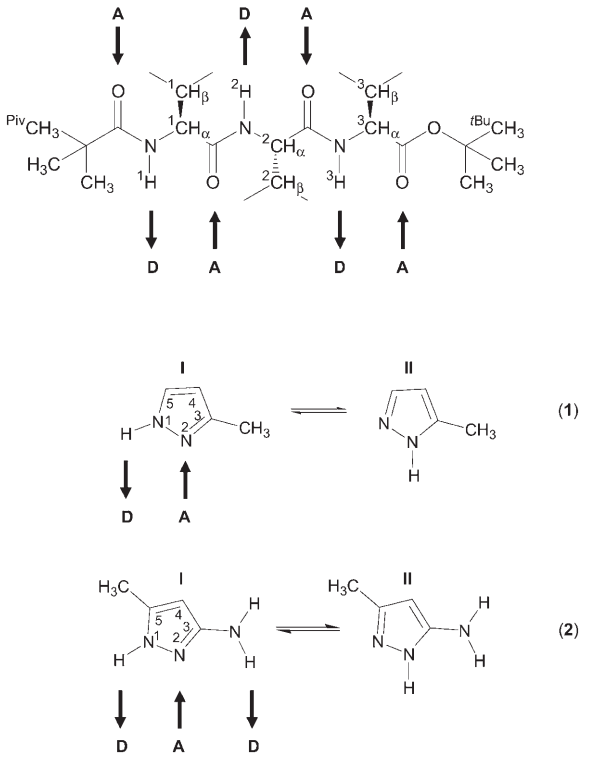

Figure 1. Structure with atom designations of the protected tripeptide Piv-Val-Val-Val-*t*Bu (top), two tautomers of 3-methylpyrazole (center) and 3-amino-5-methylpyrazole (bottom); hydrogen-bond donor (D) and acceptor sites (A) are indicated by arrows.

Direct information on the peptide conformation can be obtained from NH–CH_α vicinal coupling constants which depend on the backbone torsion angle θ. In general, coupling constants $^3J > 8$ Hz indicate a β-sheet conformation, whereas coupling constants $^3J < 6$ Hz are typical for an α-helical conformation.[13] As summarized in Table 1, coupling constants of all three amino acid residues in the tripeptide exhibit values $^3J \sim 9$ Hz and are thus compatible with an extended β-type conformation in solution at 293 K. Upon adding 3-methylpyrazole (**1**; Figure 1) in a 1:1 molar ratio, ^3J decreases by 0.3 Hz for Val-1 whereas ^3J of the central and C-terminal valine slightly increase by 0.3 Hz. In contrast, the presence of equimolar amounts of 3-amino-5-methylpyrazole (**2**) increases $^3J_{NH,CH\alpha}$ of Val-1 by 0.4 Hz but results in a decrease of the NH–CH_α vicinal coupling for valine residues 2 and 3 by 0.3 Hz. Obviously, there are some conformational adjustments in the presence of the two ligands, however, changes are rather small indicating either a preorganized peptide conformation favorable for binding or simply weak binding affinities under the conditions employed (see below).

Table 1. Association constants K_{ass} and $^3J_{NHCH\alpha}$ coupling constants for Piv-Val-Val-Val-*t*Bu with and without pyrazole ligands (1:1 molar ratio) in chloroform at 293 K.

	Val-Val-Val			Val-Val-Val + **1**			Val-Val-Val + **2**		
	^{1}NH	^{2}NH	^{3}NH	^{1}NH	^{2}NH	^{3}NH	^{1}NH	^{2}NH	^{3}NH
^3J [Hz][a]	8.8	9.1	9.1	8.5	9.4	9.4	9.2	8.8	8.8
K_{ass} [M^{-1}][b]	2.1	0.5[c]	2.4	7.1	5.1	6.4	7.1	10.7	9.2

[a] Uncertainty ± 0.1 Hz. [b] Uncertainty ≦ 10 %. [c] Uncertainty ≦ 20 %.

We have also measured the chemical shifts of the three amide protons in the peptide as a function of concentration without and with pyrazole ligands in a 1:1 molar ratio at 293 K. From these data, association constants were determined by a nonlinear least-squares-fit using a simple 1:1 association model. These are also summarized in Table 1. Obviously, there is only a weak binding of both pyrazoles to the tripeptide at ambient temperatures with $K_{ass} < 11\,M^{-1}$ for all amide protons. As expected, 3-amino-5-methylpyrazole (**2**) with its three potential hydrogen bond binding sites exhibits a somewhat higher binding affinity compared to 3-methylpyrazole (**1**). The tripeptide itself tends to weakly self-associate as evidenced by the, albeit small, concentration dependent ^{1}NH and ^{3}NH amide proton chemical shifts in the absence of the ligand. On the other hand, ^{2}NH does not seem to be significantly engaged in a hydrogen bond with an association constant $K_{ass} < 1\,M^{-1}$. Clearly, due to this self-aggregation, association constants as determined for 1:1 mixtures with the pyrazole receptors do not simply reflect ligand–peptide complexation but rather result from a combination of both homo- and heteroassociation equilibria. Note, however, that without significant hydrogen bonding of the ^{2}NH signal in a pure peptide solution, it is this central

amide proton that experiences the most noticeable increase in K_{ass} when adding **1** and in particular **2**.

To further check binding of **1** to the tripeptide, we titrated a peptide solution with **1** and followed signals of the amide protons. As shown in Figure 2 (left), titration is accompanied by downfield shifts of all three peptide NH resonances. In particular, the central ^{2}NH exhibits a significant downfield shift on adding the ligand. In contrast, adding 4-methyl-1,2,4-triazoline-3,5-dione as a control did not noticeably affect peptide NH chemical shifts (Figure 2 right). This pyrazole derivative is not expected to bind β-sheet peptides but may rather bind an α-helical conformation based on its hydrogen bond donor and acceptor pattern. Note, that all amide protons have been unambiguously assigned based on 2D NOE experiments and chemical shift differences observed between the ligand-free samples are due to differences in peptide concentration, again reflecting some hydrogen bond mediated peptide self-association.

Low-temperature NMR measurements on Piv-L-Val-L-Val-L-Val-*t*Bu: To overcome the limitations associated with a fast exchange of various conformers and/or hydrogen-bonded species in solution at ambient temperatures, we tried to reach the slow exchange regime by lowering the temperature in a low-melting freonic solvent mixture. ^{1}H NMR spectra showing the NH proton spectral region of the tripeptide dissolved in Freon are plotted as a function of temperature in Figure 3. Upon cooling, all amide protons show a downfield shift due to increased hydrogen-bond interactions. Also, significant linebroadening effects are observed at 213 K, however, NH resonances sharpen again at lower temperatures indicating slow exchange conditions. With respect to their chemical shift of δ 6.1, 6.4, and 6.2 ppm in a non-hydrogen bonded monomer (determined for $c \rightarrow 0$ in concentration-dependent measurements), ^{1}NH, ^{2}NH and ^{3}NH signals experience significant downfield shifts upon cooling to 128 K by $\Delta\delta$ of 1.5, 1.7 and 3.2 ppm, respectively. Obviously, the much larger downfield shift by ^{3}NH compared with ^{1}NH and ^{2}NH results from its preferred participation in hydrogen-bond formation.

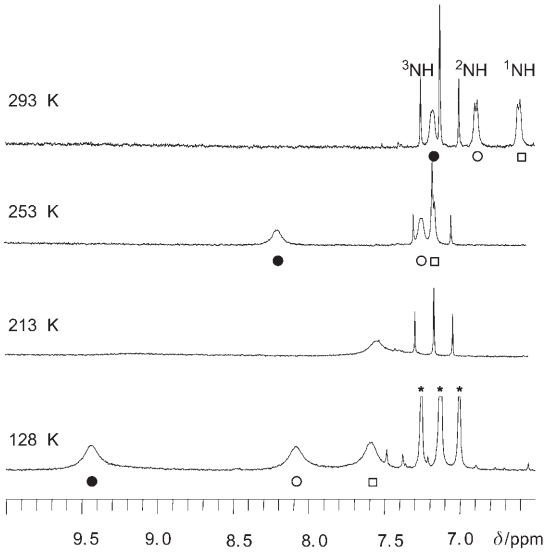

Figure 3. Temperature-dependent ^{1}H NMR spectra of Piv-Val-Val-Val-*t*Bu in Freon showing the amide proton spectral region; solvent signals are marked by asterisks at 128 K.

In order to characterize the conformation of Val-Val-Val in more detail, ^{1}H,^{1}H NOE experiments were performed under slow exchange conditions at 128 K (Figure 4). All NOE cross-peaks have the same sign as diagonal peaks indicating these arise from negative NOE values as anticipated for this temperature. NOE connectivities between protons of the tripeptide allowed the unambiguous assignment of all resonances and are summarized in Table 2. Note, that stronger interresidual $^iCH_\alpha$–$^{i+1}$NH contacts compared with intraresidual NOE values between NH and H_α-protons indicate an extended β-type conformation. A β-conformation is further corroborated by the absence of any detectable ^{i}NH–$^{i+1}$NH cross-peak.

Apparently, cross-peaks detected between ^{1}NH and ^{3}NH, ^{1}NH and the C-terminal *tert*-butyl protecting group as well as between ^{3}NH and the N-terminal pivaloyl protecting group are only compatible with a symmetric dimer through the formation of an antiparallel β-sheet conformation at low temperatures as shown in Figure 5. Four intermolecular hydrogen bonds involving the amide proton of the N- and C-terminal valine connect the two antiparallel tripeptides. However, the rather upfield shifted ^{1}NH

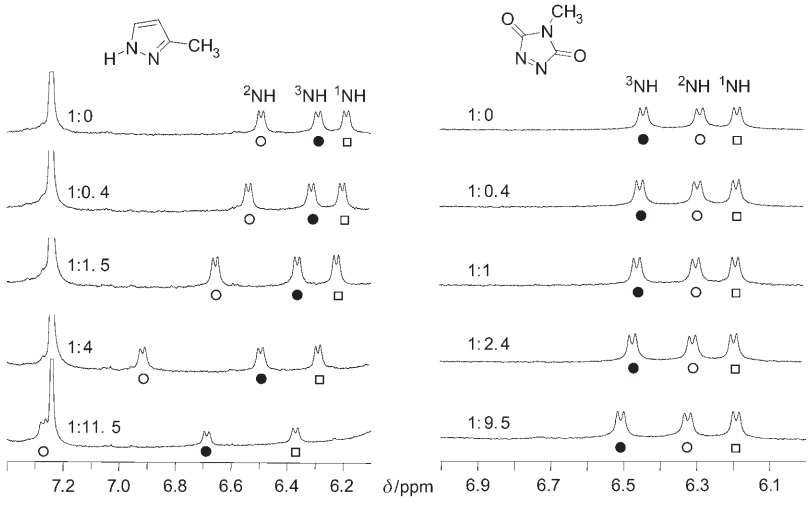

Figure 2. Amide proton spectral region of Piv-Val-Val-Val-*t*Bu at 293 K in $CDCl_3$ with different peptide/ligand molar ratios; ligand = 3-methylpyrazole (**1**; left) and 4-methyl-1,2,4-triazoline-3,5-dione (right).

Table 2. NOE interactions between protons in Piv-Val-Val-Val-*t*Bu observed in Freon at 128 K; s = strong, m = medium, w = weak.

$^{1}NH-^{Piv}CH_3$	s	$^{3}NH-^{2}CH_\alpha/^{3}CH_\alpha$	s
$^{1}NH-^{1}CH_\alpha$	w	$^{3}NH-^{3}CH_\beta$	w
$^{1}NH-^{1}CH_\beta$	w	$^{3}NH-^{2}CH_\beta$	w
$^{2}NH-^{1}CH_\alpha$	s		
$^{2}NH-^{2}CH_\alpha$	w	$^{1}NH-^{tBu}CH_3$	m
$^{2}NH-^{1}CH_\beta$	m	$^{1}NH-^{3}NH$	w
$^{2}NH-^{2}CH_\beta$	m	$^{3}NH-^{Piv}CH_3$	m

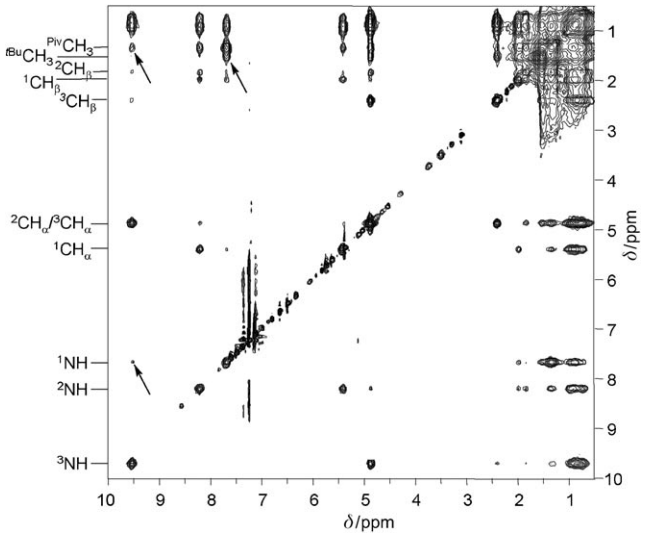

Figure 4. 2D NOE spectrum of Piv-Val-Val-Val-*t*Bu in Freon at 128 K acquired with an 80 ms mixing time; interpeptide cross-peaks are marked by arrows.

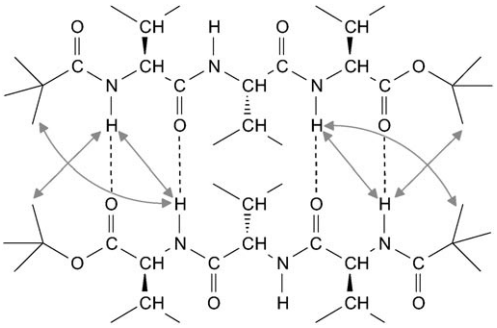

Figure 5. Piv-Val-Val-Val-*t*Bu dimer; intermolecular NOE contacts observed at low temperatures in the slow exchange regime are indicated by arrows.

proton points to a rather weak hydrogen bond due to fraying at the termini and probably some distortions caused by steric hindrance of the bulky protecting groups. Based on the absence of corresponding cross-peaks, no long-lived more extended aggregates via additional binding between individual dimers through their central amide groups are observed even at low temperatures. However, the significant downfield shift experienced by ^{2}NH upon lowering the temperature (Figure 3) suggests such weak interactions to nevertheless occur to some extent.

Low-temperature NMR studies on the complexation of Piv-Val-Val-Val-*t*Bu with pyrazole receptors: For the characterization of specific tripeptide–pyrazole interactions, 1D and 2D NMR experiments have initially been performed in Freon on a 1:1 mixture of Piv-Val-Val-Val-*t*Bu and **1**. In Figure 6 the corresponding NH proton spectral region is plotted as a function of temperature.

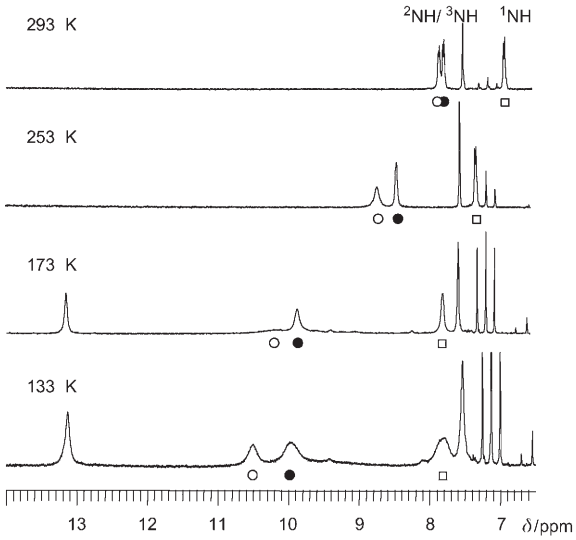

Figure 6. Temperature-dependent ^{1}H NMR spectra for a mixture of Piv-Val-Val-Val-*t*Bu and 3-methylpyrazole (1:1 molar ratio) in Freon showing the amide proton spectral region.

As for the ligand-free peptide, amide protons are downfield shifted with decreasing temperature as expected for their increased participation in the hydrogen bonding. Also, significant linebroadening effects are observed at intermediate temperatures (not shown) and persist for the central ^{2}NH proton down to 173 K before signals sharpen again at lower temperatures. Whereas ^{1}NH and ^{3}NH chemical shifts are not significantly affected by the presence of the pyrazole ligand, the ^{2}NH signal exhibits a considerable downfield shift compared with the pure tripeptide with a limiting chemical shift of $\delta(^{2}NH) = 10.5$ ppm under slow exchange conditions at 133 K. Clearly, such a behavior strongly suggests its participation in a hydrogen bond to the added pyrazole receptor. The ^{Pyr}NH signal is only observed below 193 K resonating at rather low field with $\delta(^{Pyr}NH) = 13.1$ ppm at 133 K.

Detailed structural information on the complex between the tripeptide and pyrazole **1** was obtained through a 2D NOE measurement on a 1:1 mixture of Val-Val-Val with the ligand under slow exchange conditions at 133 K (Figure 7). Observable $^{1}H-^{1}H$ NOE connectivities allow the assignment

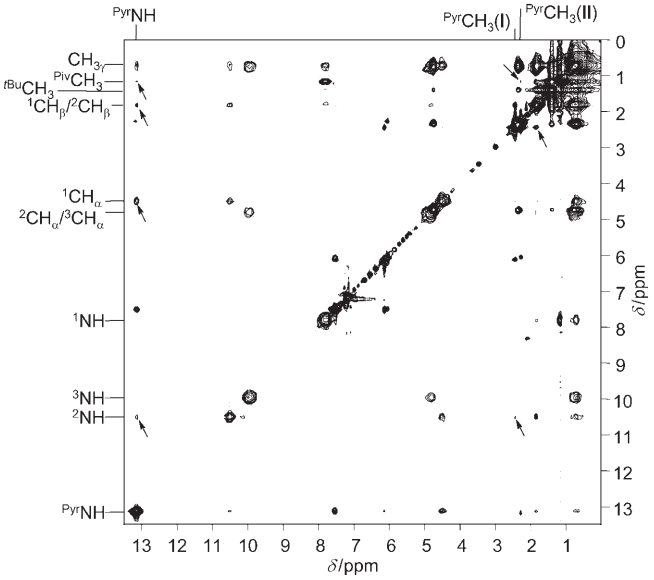

Figure 7. 2D NOE spectrum for a mixture of Piv-Val-Val-Val-*t*Bu and 3-methylpyrazole (1:1 molar ratio) in Freon acquired at 133 K with an 80 ms mixing time; NOE connectivities between peptide and ligand are indicated by arrows.

of all resonances, again indicating the formation of an extended β-conformation of the peptide in the presence of the ligand.

Although less pronounced compared with the corresponding pyrazole-free peptide, a typical intermolecular contact observed between ^{1}NH and the *tert*-butyl group at the C-terminus is only compatible with a β-sheet dimer undisrupted by the presence of the ligand. An intermolecular NOE contact between NH of pyrazole and ^{2}NH of the tripeptide points to a binding mode involving the central ^{2}NH amide proton as donor in a hydrogen bond to the ligand (Table 3). On the other hand, participation of the carbonyl oxygen of the pivaloyl group as acceptor in a hydrogen bond to the pyrazole NH is confirmed by cross-peaks of weak to medium intensity between ^{Pyr}NH and α- and β-protons of the N-terminal valine as well as to the N-terminal pivaloyl protecting group. It has to be noted, that two resolved pyrazole H4 and CH_3 resonances are observed at low temperatures demonstrating the coexistence of the two tautomers **I** and **II** (see Figure 1). Signal intensities show a 5:1 molar ratio in favor of tautomer **I** with the methyl substituent *meta*

Table 3. Intermolecular NOE interactions between protons of Piv-Val-Val-Val-*t*Bu and pyrazoles **1** and **2** observed in Freon at 133 K; s = strong, m = medium, w = weak.

Peptide–**1**		Peptide–**2**	
^{Pyr}NH–^{2}NH	w	^{Pyr}NH–^{2}NH	m
^{Pyr}NH–^{1}CH$_\alpha$	m	^{Pyr}NH–^{1}CH$_\alpha$	m
^{Pyr}NH–^{1}CH$_\beta$	w	^{Pyr}NH–^{1}CH$_\beta$	w
^{Pyr}NH–^{Piv}CH$_3$	w	^{Pyr}NH–^{Piv}CH$_3$	w
^{Pyr}CH$_3$(**I**)–^{2}NH	w	^{Pyr}CH$_3$–^{1}CH$_\alpha$	w
^{Pyr}CH$_3$(**I**)–^{2}CH$_\beta$	m	^{Pyr}CH$_3$–^{Piv}CH$_3$	w
^{Pyr}CH$_3$(**II**)–^{Piv}CH$_3$	w		

to the protonated imino nitrogen. Binding to the peptide does not influence this tautomeric equilibrium as evidenced by the same ratio in the absence of peptide. Whereas ^{Pyr}CH$_3$(**I**) exhibits NOE contacts to the centrally located ^{2}NH and ^{2}CH$_\beta$, an albeit weak contact observed between ^{Pyr}CH$_3$(**II**) and the pivaloyl group places the latter methyl substituent towards the N-terminus of the peptide as expected for the proposed binding geometry. The structure of the 2:2 complex based on the NOE data is shown in Figure 8. Note the unperturbed antiparallel dimer and the symmetric binding through two hydrogen bonds of the pyrazole ligand to the free central amide and the pivaloyl carbonyl oxygen.

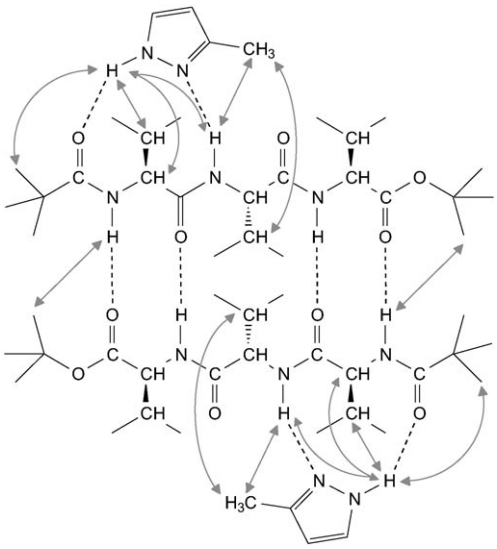

Figure 8. 2:2 complex between Piv-Val-Val-Val-*t*Bu and tautomer **I** of 3-methylpyrazole; intermolecular NOE contacts observed at low temperatures in the slow exchange regime are indicated by arrows.

The relative strengths of formed hydrogen bonds in the tetrameric associate can be derived from the downfield shifts experienced by the free amide protons upon complexation. Apparently, the largest downfield shift observed for the ^{2}NH proton engaged in hydrogen bonding to the pyrazole nitrogen acceptor must be attributed to a stronger NH···N hydrogen bond between peptide and ligand compared to the NH···O=C interpeptide hydrogen bonds. However, with only two binding sites the pyrazole derivative is unable to effectively break the dimeric tripeptide associate that is stabilized by a total of four hydrogen-bond contacts.

With its additional amino substituent, 3-amino-5-methylpyrazole (**2**) in its tautomeric form **I** may form three hydrogen bonds to either side of a monomeric tripeptide (tautomer **II** can only form two hydrogen-bond contacts to the peptide, see Figure 1). Decreasing the temperature of a peptide–aminopyrazole mixture in a Freon solution results in downfield shifts of all three amide protons as expected for their engagement in hydrogen bonding. As shown in Figure 9, the NH signal of Val-2 is again most downfield shifted at low temperatures whereas the NH resonance of

the N-terminal Val-1 only exhibits a modest shift to lower field. As before, this rather upfield shifted ^{1}NH signal can be attributed to a weakening of the interpeptide hydrogen bond due to some terminal fraying and steric hindrance of the protecting groups. Whereas the ^{Pyr}NH signal of the 3-amino-5-methylpyrazole ligand is not observed at temperatures above 200 K but sharpens upon further cooling ($\delta =$ 11.81 ppm at 128 K), resonances for the pyrazole amino protons in the range 4–5 ppm are broadened even at low temperatures (not shown). At 128 K the spectrum exhibits two additional low-intensity resonances with chemical shifts of $\delta = 11.6$ ppm and 10.9 ppm (marked by asterisks in Figure 9, see below). Notably, starting with a 1:2 peptide/ligand stoichiometric ratio, corresponding spectra upon cooling equal spectra acquired for the equimolar mixture. In fact, ligand and peptide NH signal intensities always indicate a 1:1 molar ratio at low temperatures with the precipitation of excess ligand.

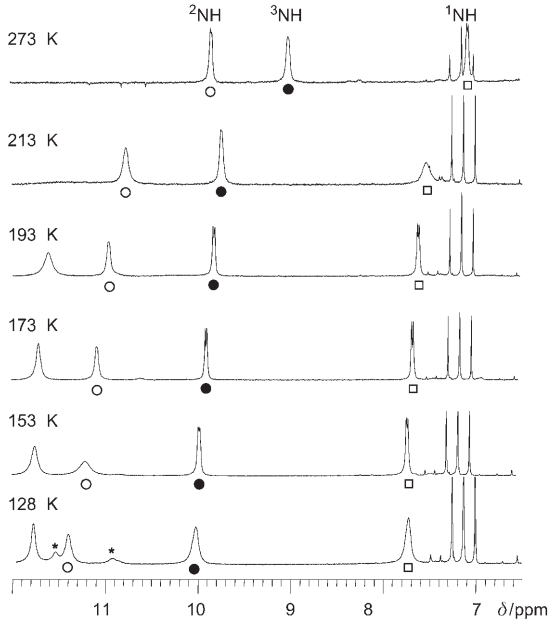

Figure 9. Temperature-dependent ^{1}H NMR spectra for a mixture of Piv-Val-Val-Val-*t*Bu and 3-amino-5-methylpyrazole (1:1 molar ratio) in Freon showing the amide proton spectral region; for the asterisks see text.

A detailed characterization of the favored complex geometry between Val-Val-Val and pyrazole **2** under slow exchange conditions is possible through 2D NOE experiments at 128 K (Figure 10). As for the free tripeptide, observed cross-peaks between ^{1}NH and ^{3}NH, ^{1}NH and $^{tBu}CH_3$ as well as ^{3}NH and $^{Piv}CH_3$ in the complex with the aminopyrazole again point to the formation of an undisrupted peptide dimer. Thus, binding of the ligand to this dimer is restricted to the available top and bottom faces with the exposed carbonyl oxygen of the pivaloyl group and the amide and carbonyl functionality of the central Val-2 as hydrogen-bond donor and acceptor sites. Note, that a strong cross-peak between ^{Pyr}NH and the pyrazole methyl substituent identifies the predominant aminopyrazole ligand as being tautomer **I** (see Figure 1). The two additional weak resonances at $\delta =$ 11.6 and 10.9 ppm exhibit contacts to ^{Pyr}NH and the peptide ^{2}NH, respectively. These cross-peaks being noticeably stronger than the corresponding diagonal signals are typical of chemical exchange and indicate the presence of a minor species possibly involving the pyrazole tautomer **II** (a minor population of tautomer **II** is also observed in a pure aminopyrazole solution at low temperatures). However, available NOE contacts do not allow a more detailed structural characterization.

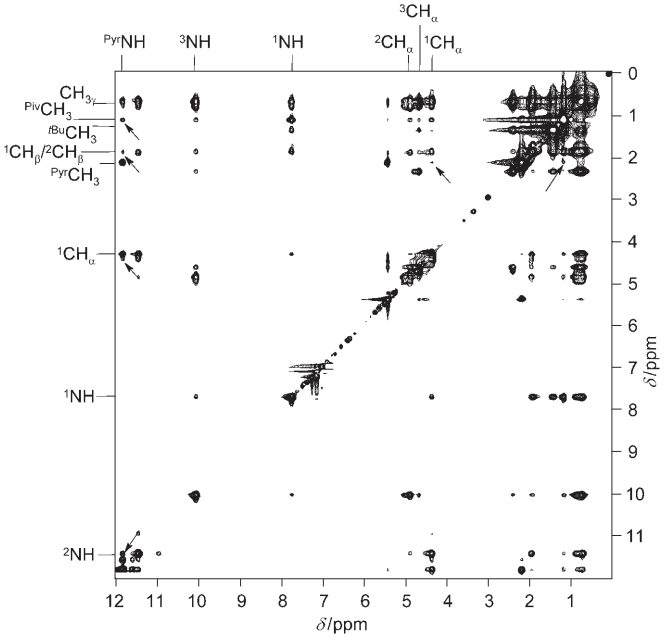

Figure 10. 2D NOE spectrum for a mixture of Piv-Val-Val-Val-*t*Bu and 3-amino-5-methylpyrazole (1:1 molar ratio) in Freon acquired at 128 K with an 80 ms mixing time; NOE connectivities between peptide and ligand are indicated by arrows.

Several characteristic NOE connectivities observed between peptide and ligand (see Table 3) places the aminopyrazole in an orientation that enables the formation of three hydrogen bonds to the available donor and acceptor sites of the peptide dimer. In particular, conspicuous intermolecular NOE contacts between ^{Pyr}NH and ^{2}NH, $^{1}CH_\alpha$, $^{1}CH_\beta$ as well as the pivaloyl protecting group again point to a hydrogen bond between CO of the pivaloyl protecting group and ^{Pyr}NH as well as between ^{2}NH and the pyrazole endocyclic nitrogen. The 2:2 complex structure in line with the NOE contacts is shown in Figure 11. Note, that the additional hydrogen bond between the amino substituent of **2** and the carbonyl group of Val-2 is not directly supported by experimental evidence but only suggested by the molecular model. In fact, broadened and rather upfield shifted NH_2 proton resonances of the pyrazole at low temperatures indicate dy-

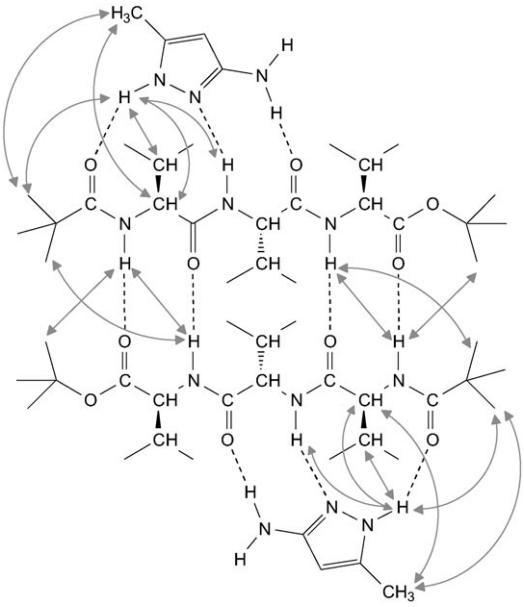

Figure 11. Structure of the 2:2 complex between Piv-Val-Val-Val-*t*Bu and 3-amino-5-methylpyrazole; intermolecular NOE contacts observed at low temperatures in the slow exchange regime are indicated by arrows.

namic exchange processes and suggest only weak hydrogen-bond interactions of the amino group.

Chemical shifts of ^{1}NH and ^{3}NH amide protons that are engaged in interpeptide hydrogen bonds are not affected by the type of complexing ligand in the slow exchange regime. Obviously, the geometry of the undisrupted peptide dimer is rather insensitive to the bound pyrazole. On the other hand, ^{2}NH in the complex with **2** is further downfield shifted by almost 1 ppm ($\delta = 11.43$ ppm) when compared to the methylpyrazole associate, pointing to a significantly stronger NH···N hydrogen bond to the aminopyrazole ligand. It may be speculated, that the somewhat higher binding affinity of the aminopyrazole **2** to the tripeptide (Table 1) results from the strengthening of this critical hydrogen bond rather than from the formation of a third hydrogen-bond contact to the pyrazole amino substituent. Excluding major geometric rearrangements, the stronger hydrogen bond is directly associated with the pyrazole endocyclic nitrogen acting as hydrogen-bond acceptor. Its acceptor capability is enhanced by the amino function and more electron-releasing substituents are expected to further strengthen the NH···N hydrogen bond between peptide and pyrazole receptors. In contrast, the donor capability of the pyrazole imino group is expected to decrease by the electronic effects of an amino group and this is indeed reflected by the obvious weakening (upfield shift) of the hydrogen bond between ^{Pyr}NH of **2** and CO of the pivaloyl protecting group. Interestingly, Hartree-Fock and DFT calculations combined with infrared/Resonant 2-Photon Ionization spectroscopy in the gas phase have recently yielded results on hydrogen bonds in clusters of a protected amino acid and pyrazole derivatives that are in line with our results on protected tripeptides in the condensed phase.[14]

Structural models for amyloid fibrils reported so far have shown a clear preference of forming parallel β-strands, yet smaller subsets of the same sequences may also form fibrils with antiparallel β-strand interactions. Factors, that govern specific interactions in the stabilization of structures (antiparallel vs parallel β-strands) and in promoting fibril formation most likely involve the specific peptide sequence but also the particular environment. Given an aprotic solvent system and low temperatures, our model system seems to be far from physiological conditions. Recent studies, however, have demonstrated the importance of backbone hydrogen bonding for the assembly of amyloid fibrils in aqueous solution. Replacing amide bonds with ester bonds has been reported to completely eliminate the aggregation of an amyloidgenic peptide.[15] The formation and strength of hydrogen bonds critically depends on the dielectric constant of the local environment and fibrillogenesis with the formation of extensive interstrand hydrogen bonds is expected to rely on hydrophobic clusters that provide for a relatively apolar microenvironment. In fact, the dielectric constant of the freonic solvent used here amounts to about 40 at 123 K, that is, higher than methanol and about half the value of water.[16] Thus, the formation of hydrogen bonded aggregates of small peptides under the low-temperature conditions in a Freon solvent is likely to follow similar rules as the formation of larger peptide aggregates in an aqueous solution.

Conclusion

The formation of stable antiparallel dimers observed for the protected tripeptide Piv-Val-Val-Val-*t*Bu through hydrogen bonding at low temperatures is promoted by the extended β-type conformation of the small peptides. Adding a pyrazole ligand will not disrupt the peptide dimer but rather results in the formation of symmetric 2:2 peptide/ligand complexes at low temperatures. Concentration- and temperature-dependent chemical shift changes of the peptide amide protons as well as NOE contacts in the presence of the pyrazoles clearly establish a bidentate hydrogen bonding to the ligand that includes CO of residue *n* and NH of residue *n*+1 Although binding of the simple pyrazoles through only two hydrogen bonds is unable to compete with peptide dimerization, capping of residual hydrogen bond donor and acceptor sites at the surface of the peptide dimer will effectively block any further aggregation. It is also important to note, that the strength of the peptide–pyrazole NH···N hydrogen bond excels the strength of corresponding peptide–peptide interactions and may be further strengthened by appropriate substituents. The studies presented are the first that provide for a detailed account of the hydrogen bond mediated affinity and geometry for pyrazoles binding to peptides in a well-defined conformation in solution. The characterization of such interactions will clearly be important for the rational design of more potent pyrazole-based ligands aimed at recognizing particular peptide conformations and thus efficient-

ly preventing pathological conditions caused by peptide aggregation.

Experimental Section

NMR measurements: NMR experiments were performed on a Bruker AMX500 spectrometer. Temperatures were adjusted by a Eurotherm Variable Temperature Unit to an accuracy of ±1.0 °C. ^{1}H chemical shifts in chloroform at 293 K were referenced relative to $CHCl_3$ (δ_H = 7.24 ppm) and in a Freon mixture relative to $CHClF_2$ (δ_H = 7.13 ppm). Concentration-dependent chemical shifts were fitted with an appropriate equation by employing the Marquardt–Levenberg algorithm. Phase-sensitive NOESY experiments were acquired using the time proportional phase incrementation (TPPI) mode with 2 K complex data points in t_2 and 1 K real data points in t_1. The NOESY data sets were apodized with a squared sine-bell function in both dimensions and Fourier-transformed to give a final matrix size of 2 K × 1 K.

Materials: 3-Methylpyrazole and 3-amino-5-methylpyrazole were purchased from Sigma-Aldrich, Munich, Germany. All reactions were controlled by TLC on silica gel plates (Merck silica gel 60 F_{254}). If necessary, solvents were dried by standard procedures prior to use. The deuterated Freon mixture $CDClF_2/CDF_3$ was prepared as described[17] and handled on a vacuum line which was also used for the sample preparation.

Piv-Val-Val-Val-OH: Pivaloyl chloride (0.24 mL) and 1 M NaOH (2 mL) were dropwise added simultaneously to a solution of H-Val-Val-Val-OH (200 mg) in 1 M NaOH (1 mL) at 0 °C. The reaction mixture was stirred for 1 h at 0 °C and 1.5 h at room temperature, then acidified with 1 M HCl. The crude product was extracted with ethyl acetate (30 mL). After drying over anhydrous Na_2SO_4, the solvent was evaporated and further drying under vacuum yielded Piv-Val-Val-Val-OH as a white solid (150 mg, 59.2 %). ^{1}H NMR (250 MHz, CD_3OD, 293 K, TMS): δ = 4.18 (m, 3H; $^1CH_\alpha$, $^2CH_\alpha$, $^3CH_\alpha$), 2.08 (m, 3H; $^1CH_\beta$, $^2CH_\beta$, $^3CH_\beta$), 1.20 (s, 9H; $OC(CH_3)_3$), 0.9 ppm (m, 18H; $3(CH(CH_3)_2)$).

Piv-Val-Val-Val-*t*Bu: Piv-Val-Val-Val-OH (150 mg) was dissolved in a mixture of dioxane (4 mL) and concentrated sulfuric acid (0.15 mL) in an 80 mL pressure bottle. Liquid isobutene (1 mL) was added and the reaction mixture was stirred for 4 h at room temperature. After the addition of a mixture of cold Et_2O (24 mL) and 1 M NaOH (15 mL), the water phase was extracted with Et_2O. The organic solution was dried over anhydrous Na_2SO_4 and evaporated under vacuum. The crude product was purified by HPLC (silica gel, CH_2Cl_2/MeOH 90:10) to yield the title compound (51 mg, 29.8 %). ^{1}H NMR (250 MHz, $CDCl_3$, 293 K, TMS): δ = 7.00 (d, 1H; ^{3}NH), 6.80 (d, 1H; ^{2}NH), 6.50 (d, 1H; ^{1}NH), 4.40 (m, 3H; $^1CH_\alpha$, $^2CH_\alpha$, $^3CH_\alpha$), 2.05 (m, 3H; $^1CH_\beta$, $^2CH_\beta$, $^3CH_\beta$), 1.48 (s, 9H; $OCO(CH_3)_3$), 1.20 (s, 9H; $OC(CH_3)_3$), 0.85 ppm (m, 18H; $3(CH(CH_3)_2)$); HR MS (80 eV, 180 °C): *m/z*: calcd for $C_{24}H_{45}N_3O_5$: 455.3359; found: 455.33472 $[M]^+$, 382.2721 $[M-OC_4H_9]^+$.

Acknowledgements

This work was supported by the Deutsche Forschungsgemeinschaft (Bonn-Bad Godesberg).

[1] a) F. Edenhofer, S. Weiss, E.-L. Winnacker, M. Famulok, *Angew. Chem.* **1997**, *109*, 1748–1769; *Angew. Chem. Int. Ed. Engl.* **1997**, *36*, 1675–1694; b) L. Dumery, F. Bourdel, Y. Soussan, A. Fialkowsky, S. Viale, P. Nicolas, M. Reboud-Ravaux, *Pathol. Biol.* **2001**, *49*, 72–85; c) R. Knight, *Proteomics* **2001**, *1*, 763–766; d) P. Kurosinski, M. Guggisberg, J. Götz, *Trends Mol. Med.* **2002**, *8*, 3–5.

[2] a) E. Zerovnik, *Eur. J. Biochem.* **2002**, *269*, 3362–3371; b) B. Austen, M. Manca, *Chem. Br.* **2000**, *36*, 28–31; c) P. T. Lansbury Jr., *Acc. Chem. Res.* **1996**, *29*, 317–321; d) B. A. Yankner, *Neuron* **1996**, *16*, 921–932.

[3] a) J. C. Rochet, P. T. Lansbury Jr., *Curr. Opin. Struct. Biol.* **2000**, *10*, 60–68; b) A. T. Petkova, Y. Ishii, J. J. Balbach, O. N. Antzutkin, R. D. Leapman, F. Delaglio, R. Tycko, *Proc. Natl. Acad. Sci. USA* **2002**, *99*, 16742–16747; c) A. T. Petkova, G. Buntkowsky, F. Dyda, R. D. Leapman, W. M. Yau, R. Tycko, *J. Mol. Biol.* **2004**, *335*, 247–260.

[4] a) M. A. Findeis, *Biochim. Biophys. Acta* **2000**, *1502*, 76–84; b) J. E. Gestwicki, G. R. Crabtree, I. A. Graef, *Science* **2004**, *306*, 865–869.

[5] a) D. S. Kemp, *Trends Biotechnol.* **1990**, *8*, 249–255; b) H. J. Schneider, *Angew. Chem.* **1993**, *105*, 890–892; *Angew. Chem. Int. Ed. Engl.* **1993**, *32*, 848–850; c) J. S. Nowick, D. M. Chung, K. Maitra, S. Maitra, K. D. Stigers, Y. Sun, *J. Am. Chem. Soc.* **2000**, *122*, 7654–7661; d) M. W. Peczuh, A. D. Hamilton, *Chem. Rev.* **2000**, *100*, 2479–2493.

[6] a) T. Schrader, C. Kirsten, *Chem. Commun.* **1996**, 2089–2090; b) C. N. Kirsten, T. H. Schrader, *J. Am. Chem. Soc.* **1997**, *119*, 12061–12068.

[7] a) M. Wehner, T. Schrader, *Angew. Chem.* **2002**, *114*, 1827–1831; *Angew. Chem. Int. Ed.* **2002**, *41*, 1751–1754; b) M. Wehner, D. Janssen, G. Schäfer, T. Schrader, *Eur. J. Org. Chem.* **2006**, 138–153.

[8] a) P. Rzepecki, M. Wehner, O. Molt, R. Zadmard, K. Harms, T. Schrader, *Synthesis* **2003**, 1815–1826; b) P. Rzepecki, L. Nagel-Steger, S. Feuerstein, U. Linne, O. Molt, R. Zadmard, K. Aschermann, M. Wehner, T. Schrader, D. Riesner, *J. Biol. Chem.* **2004**, *279*, 47497–47505.

[9] a) P. Rzepecki, H. Gallmeier, N. Geib, K. Cernovska, B. König, T. Schrader, *J. Org. Chem.* **2004**, *69*, 5168–5178; b) P. Rzepecki, T. Schrader, *J. Am. Chem. Soc.* **2005**, *127*, 3016–3025.

[10] a) A. Dunger, H.-H. Limbach, K. Weisz, *Chem. Eur. J.* **1998**, *4*, 621–628; b) A. Dunger, H.-H. Limbach, K. Weisz, *J. Am. Chem. Soc.* **2000**, *122*, 10109–10114; c) E. M. Basílio Janke, H.-H. Limbach, K. Weisz, *J. Am. Chem. Soc.* **2004**, *126*, 2135–2141; d) S. Schlund, M. Mladenovic, E. M. Basílio Janke, B. Engels, K. Weisz, *J. Am. Chem. Soc.* **2005**, *127*, 16151–16158.

[11] J. Hlavacek, K. Poduska, F. Sorm, K. Slama, *Collect. Czech. Chem. Commun.* **1976**, *41*, 1257–1264.

[12] R. W. Roeske, *Chem. Ind.* **1959**, *36*, 1121–1122.

[13] a) M. Delepierre, C. M. Dobson, F. M. Poulsen, *Biochemistry* **1982**, *21*, 4756–4761; b) H. Kessler, *Angew. Chem.* **1982**, *94*, 509–520; *Angew. Chem. Int. Ed. Engl.* **1982**, *21*, 512–523; c) K. Wüthrich, *NMR of Proteins and Nucleic Acids*, Wiley Interscience, New York, **1986**, pp. 166–168.

[14] C. Unterberg, A. Gerlach, T. Schrader, M. Gerhards, *Eur. Phys. J. D* **2002**, *20*, 543–550.

[15] D. J. Gordon, S. C. Meredith, *Biochemistry* **2003**, *42*, 475–485.

[16] I. G. Shenderovich, A. P. Burtsev, G. S. Denisov, N. S. Golubev, H.-H. Limbach, *Magn. Reson. Chem.* **2001**, *39*, S91–S99.

[17] N. S. Golubev, S. N. Smirnov, V. A. Gindin, G. S. Denisov, H. Benedict, H.-H. Limbach, *J. Am. Chem. Soc.* **1994**, *116*, 12055–12056.

Received: April 28, 2006
Published online: November 6, 2006

